

**Phân tích toàn diện phổ của berberin,  
hợp chất chính trong bài thuốc dân gian Việt Nam  
“Đại tràng hoàn Bà Giằng”**

**Nguyễn Hoàng Sa\***

*Trường Đại học Khánh Hòa, Việt Nam*

*Ngày nhận bài: 29/09/2024; Ngày sửa bài: 09/01/2025;  
Ngày nhận đăng: 20/01/2025; Ngày xuất bản: 28/02/2025*

**TÓM TẮT**

"Đại tràng hoàn Bà Giằng", một bài thuốc dân gian nổi tiếng của lương y Bà Giằng, đã được sử dụng phổ biến ở Việt Nam hơn một thế kỷ qua để điều trị viêm loét đại tràng và tiêu chảy. Trong nghiên cứu này, các mẫu thảo dược khô được chiết xuất bằng ethanol 70% để thu được dịch chiết (DTBG). Berberin, một hợp chất chính trong DTBG, đã được tách chiết bằng phương pháp sắc ký cột silica gel. Cấu trúc của hợp chất này được xác định qua phân tích phổ và so sánh với dữ liệu phổ đã công bố. Báo cáo cung cấp bình luận chi tiết về phổ của berberin, sử dụng các kỹ thuật phổ UV-Vis, FT-IR, EI-MS, 1D-NMR và 2D-NMR.

**Từ khóa:** Berberin, protoberberine alkaloid, phân tích phổ.

\*Tác giả liên hệ chính.

Email: nhoangsa@gmail.com

# Complete spectral analysis of berberine, a key compound in Vietnamese traditional remedy “Đại tràng hoàn Bà Giằng”

Nguyen Hoang Sa\*

Khanh Hoa University, Vietnam

Received: 29/09/2024; Revised: 09/01/2025;

Accepted: 20/01/2025; Published: 28/02/2025

## ABSTRACT

The traditional herbal remedy “Đại tràng hoàn Bà Giằng,” attributed to the renowned herbalist Bà Giằng, has been widely used in Vietnam for over a century, particularly for the treatment of ulcerative colitis and diarrhea. In this study, dried herbal materials were extracted using 70% ethanol, resulting in an extract known as DTBG. Berberine, a key alkaloid in DTBG, was isolated using silica gel column chromatography. Its structure was elucidated through comprehensive spectral analyses, including UV-Vis, FT-IR, EI-MS, and 1D/2D-NMR techniques. This report provides a detailed discussion of berberine’s spectral data, contributing valuable insights into the chemistry of this compound.

**Keywords:** Berberine, protoberberine alkaloid, spectral analyses.

## 1. INTRODUCTION

Vietnamese traditional medicine (VTM) has been utilized for centuries, relying heavily on herbal remedies that are perceived as safe, natural, and without significant side effects. Among the various diseases addressed by VTM, ulcerative colitis, marked by symptoms such as abdominal pain, diarrhea, rectal bleeding, and weight loss, stands out as a major health concern.<sup>1</sup> Since the early 20<sup>th</sup> century, the herbal remedy "Đại tràng hoàn Bà Giằng" (BG) has played a pivotal role in treating inflammatory bowel disease and diarrhea in traditional Vietnamese medicine.

The efficacy of BG is attributed to its rich composition of bioactive compounds, particularly alkaloids. Alkaloids are organic

compounds containing nitrogen, and they are recognized for their diverse chemical structures and broad medicinal properties. The biosynthesis of these compounds can vary significantly across plant species, contributing to their complex pharmacological effects.

BG is a traditional herbal formula composed of a variety of medicinal plants, including *Radix glycyrrhizae* (Cam thảo), *Atractylodes macrocephala* (Bạch truật), *Rhizoma coptidis* (Hoàng liên), *Saussurea lappa* (Mộc hương), *Poria cocos* (Bạch linh), *Codonopsis pilosulae* (Đẳng sâm), a fermentative herb mixture (Thần khúc), *Myristica fragrans* (Nhục đậu khấu), *Citrus reticulata* (Trân bì), *Hordeum vulgare* (Mạch nha), *Malus doumeri* (Sơn trà), *Dioscorea persimilis* (Hoài sơn), and

---

\*Corresponding author:

Email: nhoangsa@gmail.com

*Amomum villosum* (Sa nhân). Each of these plants contributes to the therapeutic potential of BG.

Several of these ingredients have shown remarkable bioactivities. For instance, *Rhizoma coptidis* (Hoàng liên) exhibits cytotoxic effects against a variety of cancer cell lines and possesses anti-proliferative properties, particularly on human esophageal cancer cells.<sup>2</sup> Its primary alkaloid constituents have also demonstrated inhibitory effects on arthritis.<sup>3</sup> Furthermore, *Atractylodes macrocephala* (Bạch truật) has been reported to inhibit nitric oxide (NO) production in activated macrophages, exhibit neuroprotective and anti-inflammatory effects, and induce apoptosis in human leukemia cells.<sup>5-8</sup>

In a recent study, we investigated the effects of the ethanol extract from BG on acute myeloid leukemia (OCI-AML) cells. The extract exhibited significant anti-cancer activity while showing no observable toxicity in acute and subchronic toxicity studies conducted on mice.<sup>9</sup>

In this study, dried powders of BG's herbal components were extracted using 70% ethanol, resulting in an ethanol extract referred to as DTBG. Berberine, a prominent alkaloid isolated from DTBG, was subjected to detailed structural characterization. This study provides a comprehensive spectral analysis of berberine, utilizing UV-Vis, FT-IR, EI-MS, and NMR techniques, including both one-dimensional and two-dimensional <sup>1</sup>H/<sup>13</sup>C NMR experiments in DMSO-d<sub>6</sub>.

## 2. METHODS

### 2.1. General

The EI-MS spectrum was recorded using an Agilent mass spectrometer. Proton nuclear magnetic resonance (<sup>1</sup>H-NMR) at 500.13 MHz and carbon-13 nuclear magnetic resonance (<sup>13</sup>C-NMR) at 125.77 MHz were performed on a Bruker Avance 500 NMR spectrometer at room temperature. Chemical shifts are reported in delta ( $\delta$ ) parts per million (ppm). Coupling constants ( $J$ ) were provided in Hertz (Hz).

### 2.2. HPLC-DAD detection of the concentrations of the DTBG

The concentration of compounds in the DTBG extract was determined using high-performance liquid chromatography with diode-array detection (HPLC-DAD). An Eclipse XDB-C<sub>18</sub> column (5  $\mu$ m, 4.6 mm  $\times$  250 mm) was used at 30 °C. The mobile phase consisted of solvent A (water with 0.1% formic acid) and solvent B (acetonitrile with 0.1% trifluoroacetic acid). A gradient elution was employed, starting with 35% solvent B and increasing to 65% over 45 minutes at a flow rate of 0.5 mL/min. The detection process lasted 60 minutes at a flow rate of 0.25 mL/min, with monitoring at 290 nm and 294 nm. The injection volume was 5  $\mu$ L. Berberine was detected with a retention time (R<sub>t</sub>) of 13.37 minutes in the HPLC chromatogram.

### 2.3. Herb materials, extraction, isolation, and purification

The herb materials used in this study were supplied by Ba Giang Pharmaceutical Company, Thanh Hoa, Vietnam. A total of 1 kg of dried "Đại tràng hoàn Bà Giangi" (BG) powder was subjected to three overnight extractions at 60 - 80°C using 70% ethanol. The resulting crude extract (DTBG) was obtained by evaporating the solvent under reduced pressure, yielding 220 g of extract. The DTBG was fractionated using silica gel column chromatography, eluted with acetone-methanol (100:5), producing eleven fractions. Fraction 5 (3.55 g) was further subjected to silica gel chromatography using acetone-methanol mixtures of increasing polarity, resulting in five subfractions. Subfraction 4 (1.27 g) underwent further purification using acetone-methanol (1:1) as the eluent. Additional purification over silica gel with acetone-methanol-acetic acid (30:30:1) produced 722 mg of raw berberine.

The raw berberine was dissolved in 10 mL of methanol, followed by the addition of five drops of concentrated hydrochloric acid while gently heating the mixture in a water bath. The resulting deep yellow solution was filtered

through a pre-warmed funnel into a pre-warmed flask. After cooling to room temperature, the solution was placed in a refrigerator at +4 °C overnight. Yellow crystals of berberine chloride formed and were collected by filtration, then washed with ice-cold methanol. The yield of berberine chloride was 565 mg, with a melting point of 195 - 197 °C.

Thin-layer chromatography (TLC) analysis of berberine was performed using *n*-butanol/cold acetic acid/water (12:3:4 v/v) as the eluent. Berberine appeared as a yellow spot with an  $R_f$  value of 0.53, exhibiting strong yellow fluorescence under UV light at 366 nm.

Berberine chloride as the ionic form  $[M^+Cl^-]$  was isolated as a yellow powder, with the following key spectroscopic data: EI-MS  $m/z$  336  $[M]^+$  (rel.% = 2.6),  $^1H$  NMR (DMSO- $d_6$ , 500.13 MHz):  $\delta_H$  9.92 (1H, s, H-8), 8.97 (1H, s, H-13), 8.21 (1H, d,  $J$  = 9.0, H-11), 8.01 (1H, d,  $J$  = 9.0, H-12), 7.81 (1H, s, H-14), 7.12 (1H, s, H-4), 6.15 (2H, s, H-2), 4.95 (1H, t,  $J$  = 6.5, H-6), 4.12 (3H, s, 9-OCH<sub>3</sub>), 4.10 (3H, s, 10-OCH<sub>3</sub>), 3.20 (1H, t,  $J$  = 6.5, H-5);

$^{13}C$  NMR (DMSO- $d_6$ , 125.77 MHz):  $\delta_C$  149.9 (C-10), 149.3 (C-3a), 147.2 (C-14a), 145.0 (C-8), 143.1 (C-9), 137.0 (C-13a), 132.5 (C-12a), 130.2 (C-4a), 126.2 (C-11), 123.0 (C-12), 120.9 (C-13b), 120.0 (C-8a), 119.7 (C-13), 107.8 (C-4), 104.8 (C-14), 101.5 (C-2), 61.5 (C-15), 56.4 (C-16), 54.7 (C-6), 25.8 (C-5).

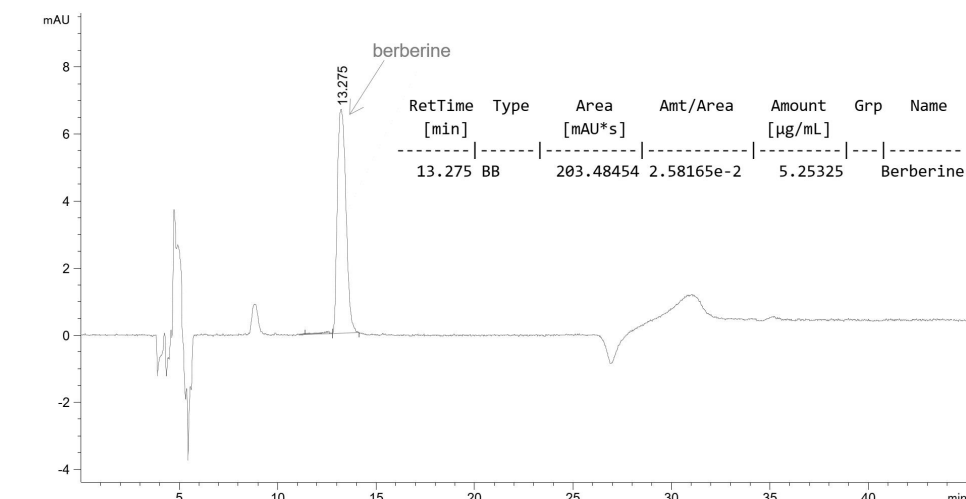


**Figure 2.** HPLC analysis of berberine, with the mobile phase composed of ACN-H<sub>2</sub>O:0.1% TFA in linear gradient mode over 0-45 minutes, at a flow rate of 1.5 mL/min.

### 3. RESULTS AND DISCUSSION

The isolated compound's structure was identified as berberine by comparing its spectral data with reference literature.<sup>10,11</sup> Berberine belongs to the class of protoberberine alkaloids, which are part of the isoquinoline alkaloid group. These alkaloids often occur as protoberberinium salts, such as berberine or berberine chloride, or as tetrahydroprotoberberines. Berberine is well-known for its bright green-yellow fluorescence, which is utilized in histological staining to visualize heparin in mast cells under fluorescence microscopy.

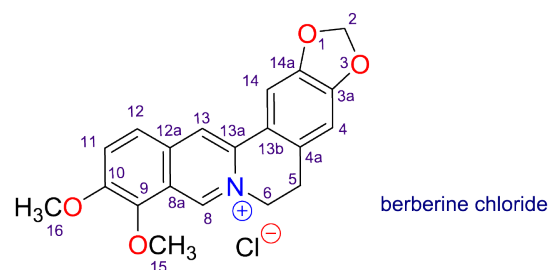


**Figure 1.** Structures of berberine chloride.

Figure 2 presents the HPLC analysis of the purified berberine from DTBG. The purity of the isolated compound was determined to be 98.7%. HPLC analysis was also used to quantify key marker compounds, including berberine, within the DTBG extract. The analysis revealed that berberine content in DTBG was approximately 0.63%, as shown in Figure 3.

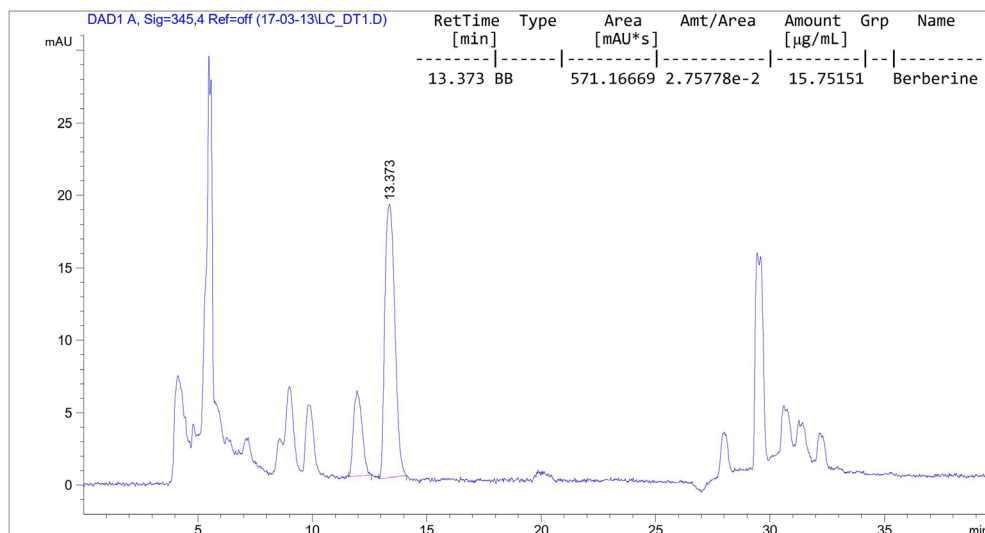


**Figure 3.** HPLC chromatogram of berberine from DTBG, using the same mobile phase and flow rate conditions.

The most deshielded proton signal at  $\delta_{\text{H}}$  9.92 is assigned to H-8 due to its proximity to the positively charged nitrogen atom (N). Similarly, the signal at  $\delta_{\text{H}}$  8.97 is attributed to H-13 in the same aromatic ring (Figure 4). The proton signals at  $\delta_{\text{H}}$  8.21 and 8.01 form an AB-spin system with a coupling constant ( $J$ ) of 9.0 Hz, which is characteristic of aromatic protons H-11 and H-12. The NOESY spectrum (Figure 5) helps differentiate these signals, with  $\delta_{\text{H}}$  8.21 showing a nuclear Overhauser effect

(NOE) contact with a methoxy group at  $\delta_{\text{H}}$  4.10, thereby confirming its assignment to H-11. By deduction, the methoxy signal corresponds to H-16. The singlets at  $\delta_{\text{H}}$  7.81 and 7.12 are assigned to H-14 and H-4, respectively. NOESY analysis confirms this assignment through an NOE contact between H-13 and H-14. The singlet at  $\delta_{\text{H}}$  6.15, corresponding to two protons, is assigned to H-2 based on its chemical shift. Multiple signals at  $\delta_{\text{H}}$  4.95 and  $\delta_{\text{H}}$  3.20 are attributed to methylene protons H-6 and H-5, respectively.

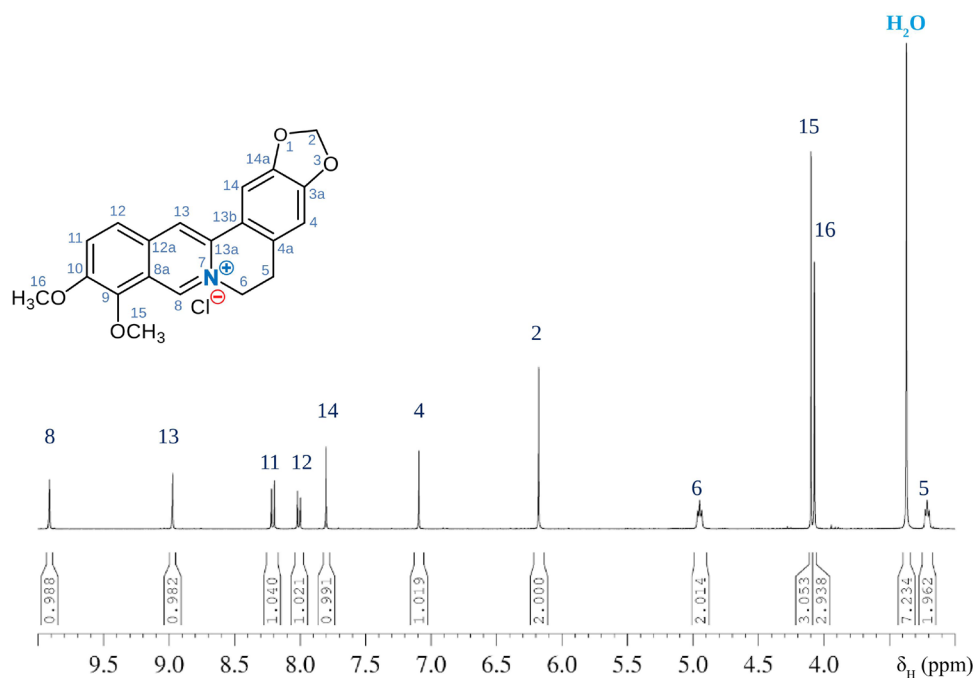


**Figure 4.**  $^1\text{H}$ -NMR of berberine chloride in  $\text{DMSO-d}_6$ .

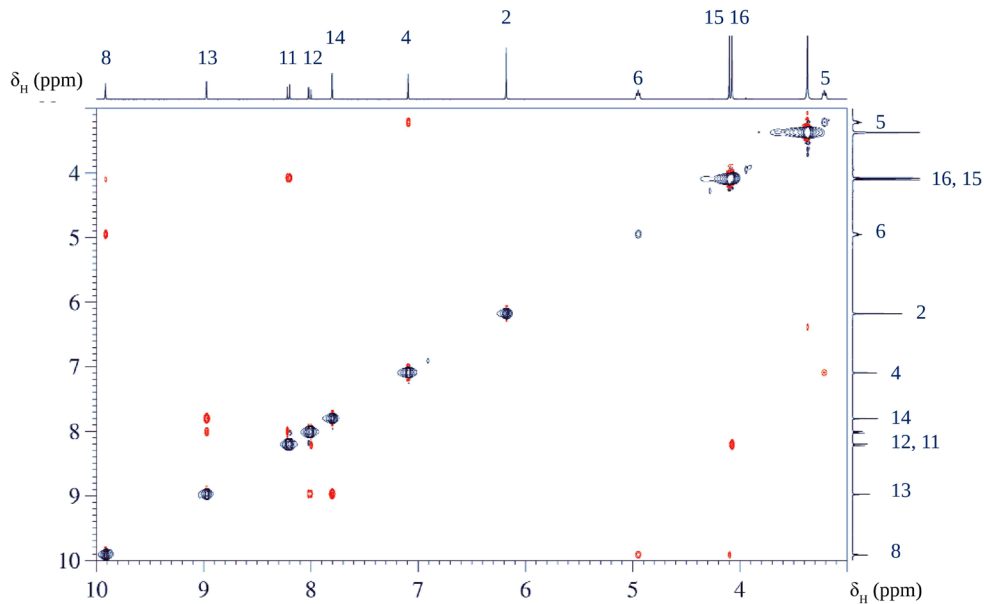


**Figure 5.** NOESY of berberine chloride.

Having fully assigned the proton signals, the carbon atoms carrying these protons can be identified using the HSQC spectrum (Figure 6). However,  $^{13}\text{C}$  chemical shifts are influenced by the solvent, potentially causing minor discrepancies in assignments. The values recorded in  $\text{DMSO-d}_6$  (Figure 7) are consistent with those reported by Blasko et al.<sup>10</sup> Quaternary carbon atoms, which lack direct proton attachments, are more challenging to assign and often require HMBC analysis for confirmation.

From H-8, we expect five HMBC correlations (Figure 8 and Figure 9): three-bond correlations with C-6, C-13a, C-12a, and C-9, and a two-bond correlation with C-8a. C-9 should also correlate with the methoxy protons (H-15), confirming that the signal at  $\delta_{\text{C}}$  143.1 is assigned to C-9. Similarly, H-11 correlates with C-12a, leading to the assignment of the signal at  $\delta_{\text{C}}$  132.5 for C-12a. C-13a is correlated with H-14, assigning the signal at  $\delta_{\text{C}}$  137.0 to C-13a.

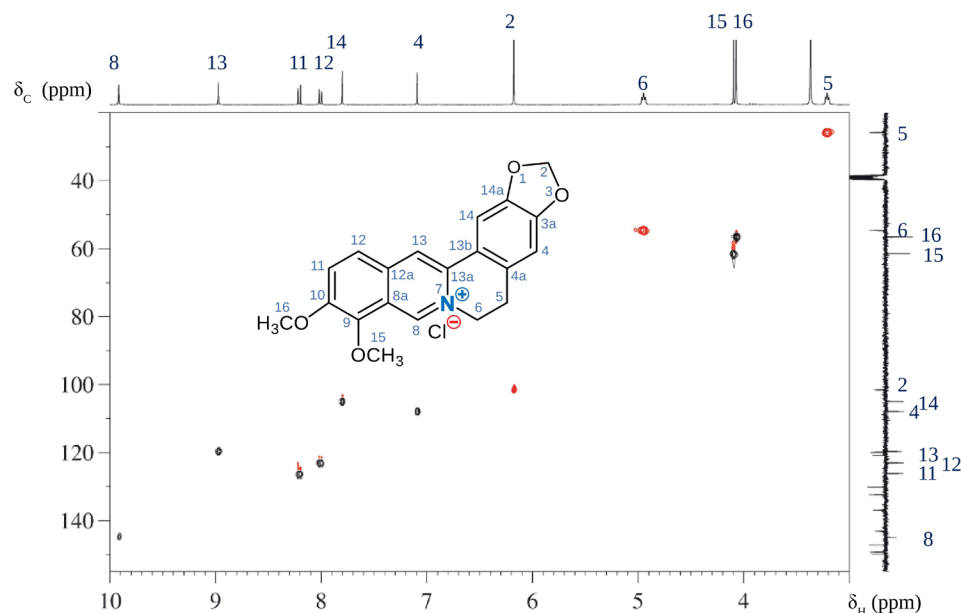


**Figure 6.** HSQC of berberine chloride.

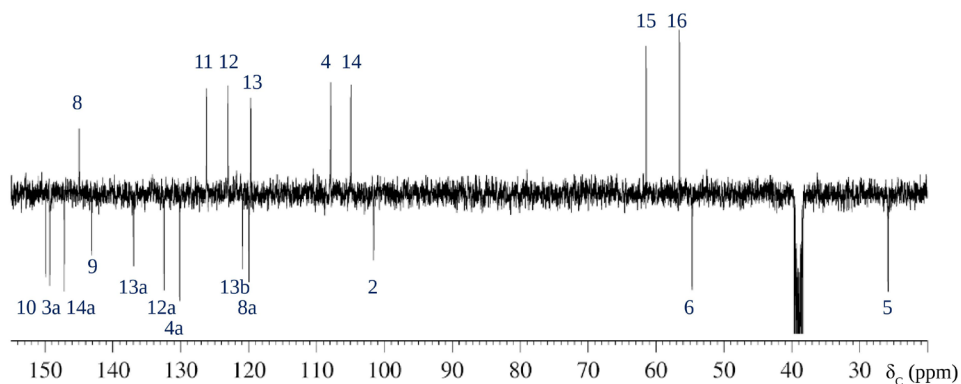


**Figure 7.** APT  $^{13}\text{C}$ -NMR of berberine chloride.

C-8a correlates with both H-12 and H-13, supporting the assignment of the signal at  $\delta_{\text{C}}$  120.0 to C-8a. All five HMBC correlations for H-8 are now assigned. In the linear annulated aromatic ring, the only remaining unassigned quaternary carbon is C-10, which can be identified via correlations with H-16 and H-12, giving the signal at  $\delta_{\text{C}}$  149.9. The remaining quaternary carbon signals are from C-4a, C-13b, C-14a, and C-3a, all part of the isolated aromatic ring. C-3a correlates with H-2 and H-14, corresponding to the signal at  $\delta_{\text{C}}$  149.3. C-14a, linked to H-2 and H-4, corresponds to the signal at  $\delta_{\text{C}}$  147.2. C-13b correlates with H-13 and H-4, producing

the signal at  $\delta_{\text{C}}$  120.9, while C-4a is assigned via correlations with H-14 and H-6 to  $\delta_{\text{C}}$  130.2.

The UV-Vis spectrum of berberine chloride (Figure 10) exhibits three prominent absorption peaks at 227 nm, 252 nm, and 354 nm, with logarithmic molar absorptivity ( $\lg\epsilon$ ) values of 0.750, 0.745, and 0.740, respectively. Additionally, a weaker absorption band is observed at 423 nm with a  $\lg\epsilon$  value of 0.15. These absorption bands, known as B bands, correspond to forbidden  $\pi$ -electron transitions ( ${}^1\text{A}_{1g} \rightarrow {}^1\text{B}_{2u}$ ) commonly associated with aromatic systems containing benzene rings or six-membered heteroaromatic rings.

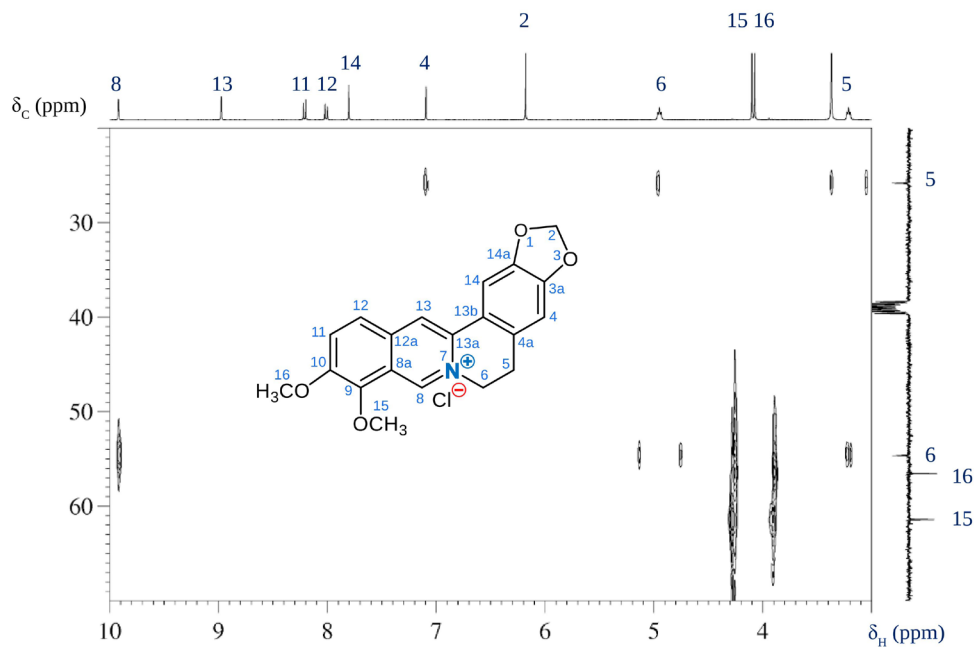


**Figure 8.** HBMC of berberine chloride in the aliphatic  $^{13}\text{C}$  region.

The absorption observed in the blue region of the visible spectrum contributes to the compound's characteristic yellow coloration. The conjugated  $\pi$ -system of berberine chloride experiences a bathochromic shift, attributed

to the electronic effects of four auxochromic oxygen substituents and the positively charged quaternary nitrogen atom. This shift highlights the impact of the molecule's structural features on its electronic transitions and optical properties.

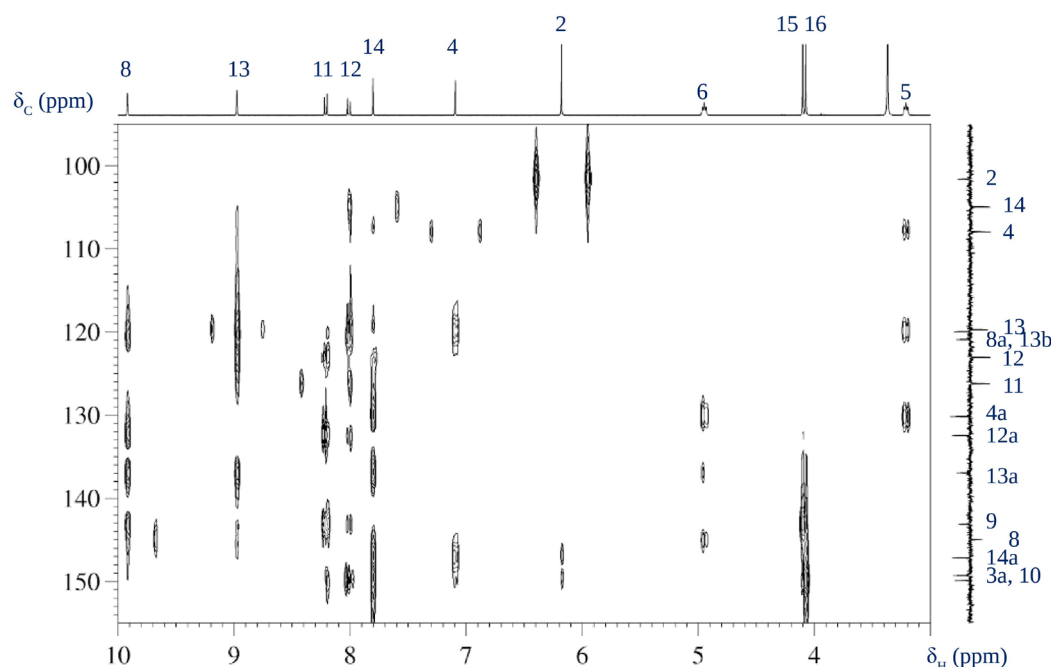


**Figure 9.** HBMC of berberine chloride in the aromatic  $^{13}\text{C}$  region.

The crystallization of berberine chloride with four water molecules explains the strong O—H vibrational band observed at 3500-3200  $\text{cm}^{-1}$  in the FT-IR spectrum (Figure 11). The C—H stretching region reveals the presence

of both  $sp^3$  and  $sp^2$  hybridized carbon atoms, while the broad band at 1630  $\text{cm}^{-1}$  is attributed to the C=N vibration. The sharp bands observed between 1600 and 1450  $\text{cm}^{-1}$  correspond to the C=C stretching of the aromatic rings.

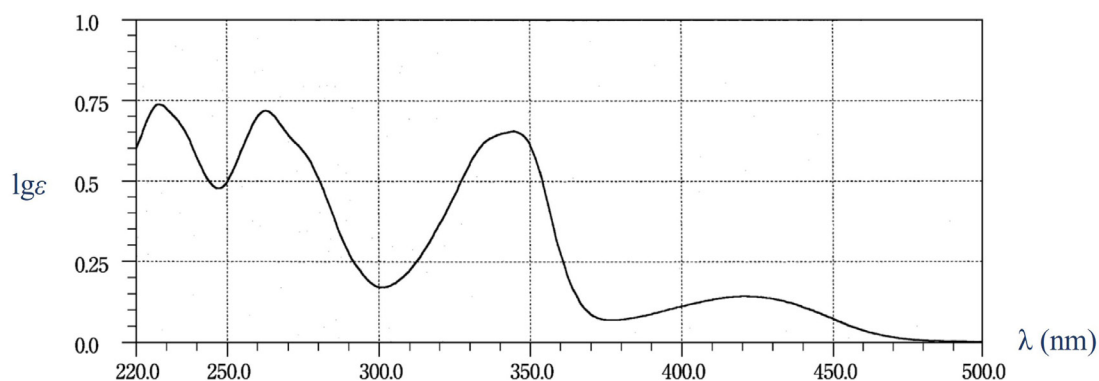


**Figure 10.** UV-Vis of berberine chloride.

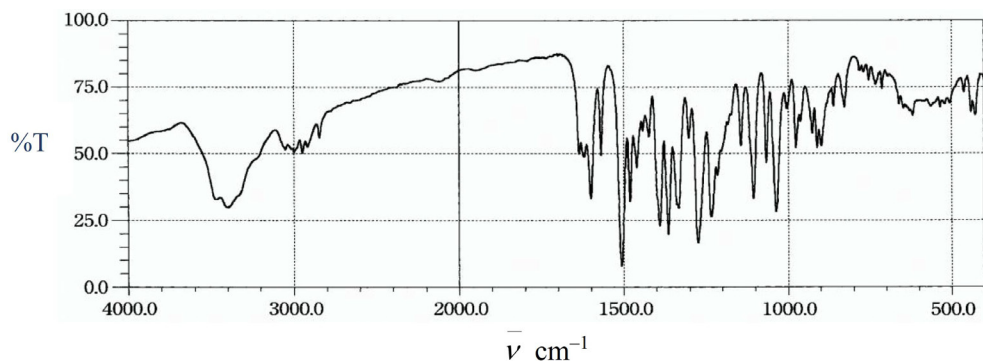


**Figure 11.** FT-IR of berberine chloride in KBr.

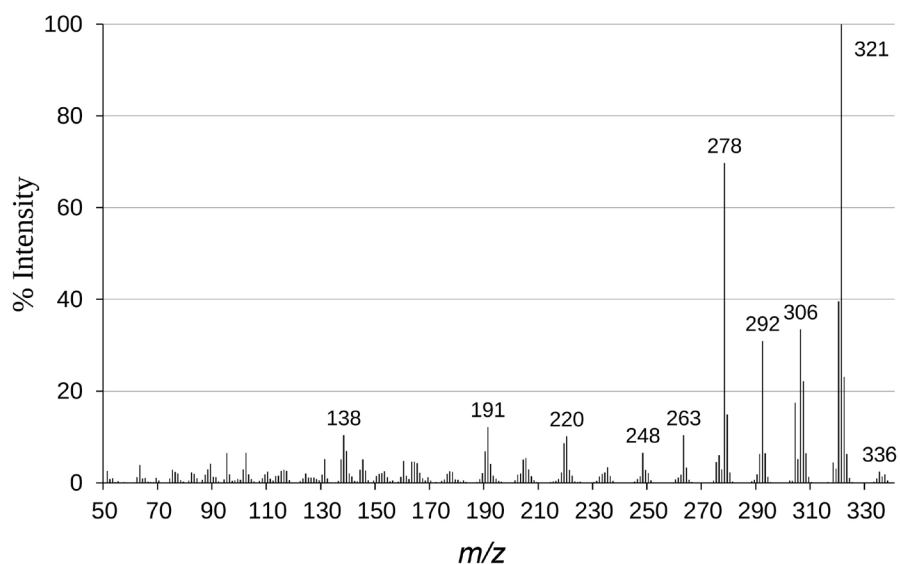


**Figure 12.** EI-MS of berberine chloride.

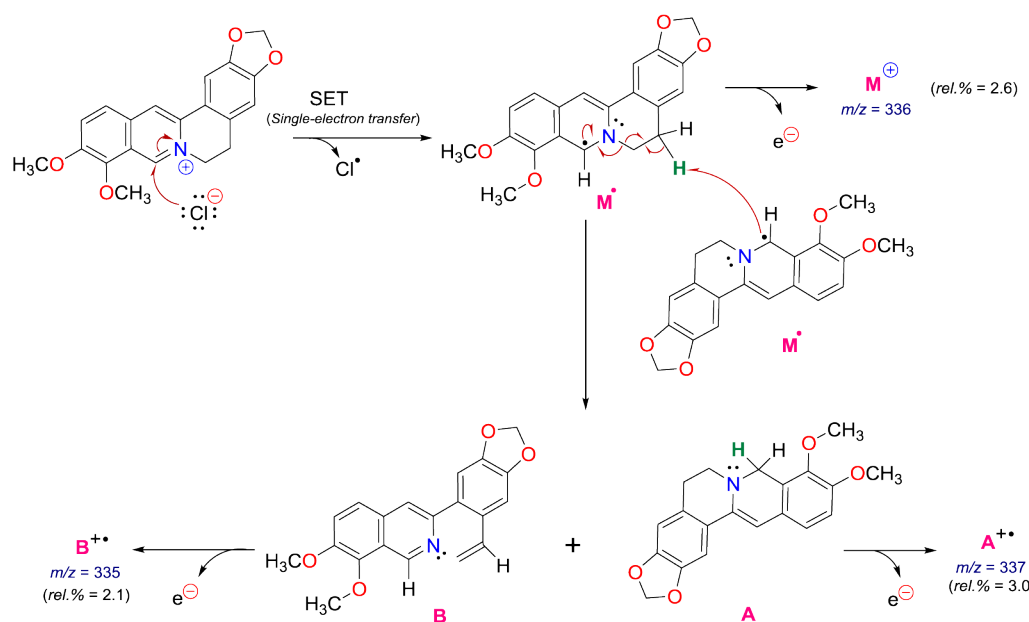


**Figure 13.** Electron transfer mechanism in the ionization source,  $\mathbf{M}^+$  ( $m/z$  336),  $\mathbf{A}^{+\cdot}$  ( $m/z$  337), and  $\mathbf{B}^{+\cdot}$  ( $m/z$  335).

The mass spectrum (Figure 12) reveals the formation of several ions through an electron transfer process in the inlet system. The cation  $M^+$  ( $m/z$  336) generated from berberine chloride undergoes radical formation ( $M^{\cdot}$ ), followed by the loss of an electron, resulting in the ion detected at  $m/z$  336. Two additional ions at  $m/z$  335 and 337 are formed through disproportionation reactions,

producing neutral molecules A and B, which are subsequently ionized (Figure 13).

Other prominent ions at  $m/z$  320, 304, 292, and 278 are likely generated through a common cleavage mechanism. These ions, having an even number of electrons, follow similar fragmentation pathways, as outlined in Figure 14.

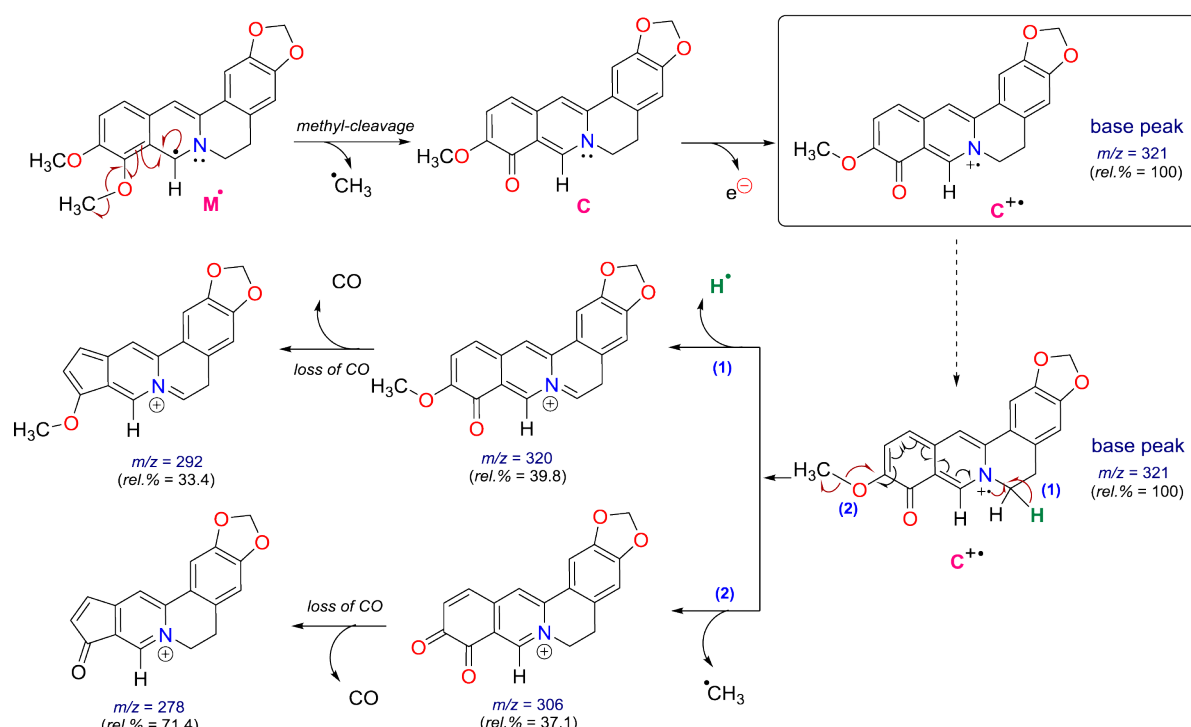


**Figure 14.** Cleavage of a methyl group from radical  $M^{\cdot}$ , leading to the formation of a neutral molecule **C** and its corresponding fragment ions.

#### 4. CONCLUSION

In summary, the  $^1\text{H-NMR}$  and  $^{13}\text{C-NMR}$  spectra of berberine chloride have been fully assigned. Comprehensive signal interpretation was conducted using various  $^2\text{D-NMR}$  spectroscopies: HSQC, NOESY, and HMBC. Furthermore, supplementary techniques, including UV-Vis, FT-IR, and EI-MS, were utilized, yielding precise data for the thorough structural elucidation of berberine.

#### REFERENCES

1. R. J. Xavier, D. K. Podolsky. Unravelling the pathogenesis of inflammatory bowel disease, *Nature*, **2007**, 448(7152), 427-434.
2. B. L. Ma, Y. M. Ma, R. Shi, T. M. Wang, N. Zhang, C. H. Wang, Y. Yang. Identification of the toxic constituents in *Rhizoma Coptidis*, *Journal of Ethnopharmacology*, **2010**, 128(2), 357-364.
3. N. Iizuka, K. Miyamoto, K. Okita, A. Tangoku, H. Hayashi, S. Yosino, T. Abe, T. Morioka, S. Hazama, M. Oka. Inhibitory effect of *Coptidis Rhizoma* and berberine on the proliferation of human esophageal cancer cell lines, *Cancer Letters*, **2000**, 148(1), 19-25.
4. X. Zhou, X. Lin, Y. Xiong, L. Jiang, W. Li, J. Li, L. Wu. Chondroprotective effects of palmatine on osteo arthritis in vivo and *in vitro*: a possible mechanism of inhibiting the Wnt/ $\beta$ -catenin and Hedgehog signaling pathways, *International Immunopharmacology*, **2016**, 34, 129-138.

5. C. M. Yao, X. W. Yang. Bioactivity-guided isolation of polyacetylenes with inhibitory activity against NO production in LPS-activated RAW264.7 macrophages from the rhizomes of *Atractylodes macrocephala*, *Journal of Ethnopharmacology*, **2014**, 151(1), 791-799.
6. N. Zhang, C. Liu, T. M. Sun, X. K. Ran, T. G. Kang, D. Q. Dou. Two new compounds from *Atractylodes macrocephala* with neuroprotective activity, *Journal of Asian Natural Products Research*, **2017**, 19(1), 35-41.
7. L. S. Hoang, M. H. Tran, J. S. Lee, T. Q. M. Ngo, M. H. Woo, B. S. Min. Inflammatory inhibitory activity of Sesquiterpenoids from *Atractylodes macrocephala* Rhizomes, *Pharmaceutical Society of Japan*, **2016**, 64(5), 507-511.
8. H. L. Huang, T. W. Lin, Y. L. Huang, R. L. Huang. Induction of apoptosis and differentiation by atactylenolide-1 isolated from *Atractylodes macrocephala* in human leukemia cells, *Bioorganic and Medicinal Chemistry Letters*, **2016**, 26(8), 1905-1909.
9. N. H. Sa, T. T. Thuy, T. D. Quan, D. D. Thien, N. T. Tam, L. C. Hoan, L. T. H. Nhung, H. T. N. Ni, S. Adorisio, D. V. Delfino. The alkaloids and bioactivities of ethanol extract from a traditional remedy of Vietnam, *The Natural Products Journal*, **2020**, 10(1), 20-25.
10. G. Blaskó, G. A. Cordell, S. Bhamarapravati, C. W. W. Beecher. Carbon-13 NMR assignments of Berberine and Sanguinarine, *Heterocycles*, **1988**, 27, 911-916.
11. L. Grycová, J. Dostál, R. Marek. Quaternary protoberberine alkaloids, *Phytochemistry*, **2007**, 68(2), 150-175.



© 2025 by the authors. This Open Access Article is licensed under the Creative Commons Attribution-NonCommercial 4.0 International (CC BY-NC 4.0) license (<https://creativecommons.org/licenses/by-nc/4.0/>).